Journal of Paleontological Techniques

Number 14 May 2016

PHOTOGRAMMETRY VS. MICRO-CT SCANNING FOR 3D SURFACE GENERATION OF A TYPICAL VERTEBRATE FOSSIL - A CASE STUDY

Julia M. Fahlke[1] and Marijke Autenrieth[1]

1 - Museum für Naturkunde, Leibniz-Institut für Evolutions- und Biodiversitätsforschung, Invalidenstraße 43, 10115 Berlin, Germany
E-mail: Julia.Fahlke@mfn-berlin.de

ABSTRACT

Over the recent years, three-dimensional (3D) surface digitization of fossils has achieved wide application in vertebrate paleontology, be it for reconstruction, morphometric or preservation purposes. The wide array of techniques available for 3D surface generation can, however, be somewhat confusing. Therefore, the aim of our study is to help the paleontologist reach a well-informed decision on which technique to use for standard purposes, taking into account aspects such as accuracy, reproducibility, and efficiency. In this study, we are comparing the above aspects when applying micro-computed tomography (micro-CT), manual photogrammetry and automated photogrammetry to an object typically digitized in vertebrate paleontology: a medium-sized fossil mammal cranium (that of an early Oligocene anthracotheriid). Our results show that manual photogrammetry has a high degree of reproducibility and is the most efficient, least costly method of the ones tested, although more training is required for the unexperienced researcher. Also, when attention is paid to proper lighting and overlap, fewer photographs do not necessarily yield inaccurate results, increasing the speed of data acquisition even more. Disadvantages of CT scanning in external surface generation include the lack of a photo surface, and long post-processing times due to removal of internal surface structures that are not used for this purpose. The technology used for automated photogrammetry, MDS Witikon, offers fast and convenient digitization. Large amounts of data and detail produced, however, may be very useful for the creation of object panoramas but exceed the limits for common use of 3D surfaces.

Keywords: Digitization; accuracy; efficiency; CloudCompare; Bothriodontinae; Anthracotheriidae

RESUMO [in Portuguese]

Recentemente, a digitalização da superfície de fósseis a três dimensões (3D) tem tido uma ampla aplicação na paleontologia de vertebrados, quer para propósitos de reconstrução, morfometria ou preservação. O vasto espectro de técnicas disponíveis para a geração de superfícies 3D pode, no entanto, ser confusa. Portanto, o objectivo deste estudo é ajudar o paleontólogo a chegar a uma decisão bem informada sobre que técnica usar para propósitos normais, tendo em consideração a precisão, reprodutibilidade e eficiência. Neste estudo, comparamos os aspectos acima quando usando tomografia computorizada, fotogrametria manual e fotogrametria automática para um objecto tipicamente digitalizado em paleontologia de vertebrados: um crânio de um mamífero fossilizado (Anthracotheridae do Oligocénico inferior). Os nossos resultados demonstram que a fotogrametria manual tem um elevado grau de reprodutibilidade, é mais eficiente e menos caro dos métodos testados, apesar de requerer mais treino para um investigador com pouca experiência. Além disso, quando a atenção devida é tomada à luz e sobreposição, menos fotografias não implicam piores resultados, o que aumenta a velocidade de aquisição. As desvantagens da tomografia computorizada para fins de geração de modelos da superfície externa incluem a ausência de uma foto de superfície bem como um pós-processamento demorado devido à remoção das estruturas internas desnecessárias. A tecnologia usada para fotogrametria automática, MDS Witikon, oferece uma digitalização rápida e conveniente. Grandes quantidades de informação e detalhe são produzidos, contudo, apesar de ser útil para a criação de *object panoramas* mas excede os limites para o uso comum de superfícies 3D.

How to cite this paper: Fahlke, J.M. and Autenrieth, M. (2016). Photogrammetry vs. Micro-CT scanning for 3D surface generation of a typical vertebrate fossil – A case study. Journal of Paleontological Techniques, 14:1-18.

Copyright (c) 2016 by Fahlke and Autenrieth. This work is made available under the terms of the Creative Commons Attribution 3.0 Unported License, http://creativecommons.org/licenses/by-sa/3.0/.

INTRODUCTION

Over the past two decades or so, 3D digitization of vertebrate fossils has become increasingly common, and nowadays 3D surface models are widely used for research, exhibition, and archiving purposes. Various digitization methods exist, the ones most commonly used in vertebrate paleontology probably being x-ray CT (including micro-CT), laser scanning (stationary or hand-held), and photogrammetry. This variety presents the researcher with the difficult decision of which method to choose for their specific purpose. For reviews of the individual methods including their history, applications in paleontology, advantages and limits, see Mallison (2011) and Sutton et al. (2014).

The aim of this study was to compare two major methods, photogrammetry and micro-CT scanning in terms of accuracy, reproducibility, and efficiency, and thereby to help researchers choose the appropriate method for their purposes. Accuracy and reproducibility were assessed by testing for three aspects: 1. similarity of surfaces generated from micro-CT scans vs. photogrammetry, 2. inter-user error when surfaces are reconstructed from the same data set (micro-CT) using different computer programs and settings, and 3. error when using the same method (photogrammetry) on photographs taken by different people. Efficiency was addressed by evaluating the duration of individual steps of surface generation, and by also taking into account the costs and the learning process of the different methods.

We chose to use this particular specimen, a cranium of an early Oligocene bothriodontine anthracotheriid, because it represents the kind of object vertebrate paleontologists typically have to deal with when generating 3D surfaces: skulls and skeletons, or parts thereof. These highly complex objects feature foramina, fossae, processus, and sharp cristae that contain a lot of morphological information. Detailed visualization of this information in the 3D model is usually crucial for subsequent morphometric or other analyses. Our specimen is intermediate in size between very small (e.g., micromammals) and very large vertebrate fossils (e.g., dinosaurs), and thus serves well as a general model specimen.

Figure 1 - The cranium of Bothriodontinae indet. (MB.Ma. 51832). A) Dorsolateral view. B) Ventrolateral view. Scale bar is 10 cm.

THE SPECIMEN

The anthracotheriid cranium used in this study was found in South Dakota and is housed at the Museum für Naturkunde Berlin, Germany (collection number MB.Ma. 51832; Figure 1). The specimen is exceptionally well-preserved in that the cranium is virtually complete, except for missing front teeth and some damage to the basisphenoid. Post-mortem deformation is restricted to a slight leftward shear that includes some dorso-ventral compression of the right side of the cranium. Condylo-basal length is 37.5 cm.

MB.Ma. 51832 has not been formally described yet but is labelled as "*Bothriodon americanus*". The presently valid species name would be *Aepinacodon americanus* (Kron and Manning, 1998; Lihoreau and Ducrocq, 2007). However, *A. americanus* is late Eocene in age. If the age information on our specimen, early Oligocene, is correct, then it is possible we are dealing with *Bothriodon rostratus* instead. But since the present study is purely technical, description and assignment of the specimen on the species level are beyond the scope of this paper. *Aepinacodon* and *Bothriodon* are likely sister taxa within the Bothriodontinae (Lihoreau and Ducrocq, 2007). Therefore, we decided to refer to our specimen as Bothriodontinae indet. here.

Bothriodontine anthracotheriids possibly lived along river banks in swamp-like environments, a potential semi-aquatic lifestyle being discussed controversially (Clark et al., 1967; Kron and Manning, 1998). They may have been forest-dwelling browsers, or possibly generalist feeders (Kron and Manning, 1998; Lihoreau and Ducrocq, 2007; cf. Janis, 1995).

METHODS

In this section, settings and programs used on each dataset as well as the conduction of the comparisons are described. Documentation of the learning process and practicing times before successful application by MA was part of the evaluation of each method. Surface names, methods and programs used, and duration of 3D surface generation and processing are summarized in Table 1 for all models.

Photographs and surface files are available for download at https://figshare.com/s/73c651841e9b3271d9ee. Further files related to this study are stored at the Museum für Naturkunde Berlin and can be made available by the corresponding author upon request.

Micro-CT scanning

The cranium MB.Ma. 51832 was scanned in two segments at the Steinmann-Institut, University of Bonn, Germany, using a micro-CT scanner (GEphoenix|X-ray v|tome|x s). Isometric voxel length was 0.246370 mm. Image stacks of two scans were registered based on gray values and transformed to a single file using Amira 5.0 software.

Table 1 - Users, methods and programs used, and duration of individual steps of 3D model generation. *CT surface generation times reflect the complete duration from opening image stacks to finished surface extraction, including registration of CT data sets. **Surface generation settings in PhotoScan were chosen to limit face count.

Surface name	Method	Number of photos	Data collected by	Surface generated by	Post-processing done by	Program used for model generation	Program used for post-processing	Data collection time (hrs)	Surface generation time (hrs)	Post-processing time (hrs)	Initial face count	Final face count
CT_JMF	micro-CT	n.a.	Steinmann-Institut Bonn	Julia M. Fahlke	Julia M. Fahlke	Amira 5.0	GOM Inspect v.7.5	4,5	6,3*	6,3	760939 (anterior), 1015221 (posterior)	750000
CT_MA	micro-CT	n.a.	Steinmann-Institut Bonn	Marijke Autenrieth	Marijke Autenrieth	ZIB-Amira 2015.24	Geomagic Studio 10	4,5	9,8*	17,0	6588084	750000
P_MA	manual photogrammetry (ring flash)	378	Marijke Autenrieth	Marijke Autenrieth	Marijke Autenrieth	Agisoft PhotoScan Professional 1.2.0	Geomagic Studio 10	1,0	10,0	2,0	999999**	750000
P_HM	manual photogrammetry (built-in flash)	150	Heinrich Mallison, Berlin	Marijke Autenrieth	Marijke Autenrieth	Agisoft PhotoScan Professional 1.2.0	Geomagic Studio 10	0,5	9,0	2,5	3217118	750000
P_JMF	manual photogrammetry (no flash)	83	Julia M. Fahlke	Marijke Autenrieth	Marijke Autenrieth	Agisoft PhotoScan Professional 1.2.0	Geomagic Studio 10	0,3	6,0	1,5	1000000**	750000
WITI	MDS Witikon (external flash)	576	EDICO SK, Bratislava	EDICO SK, Bratislava	Marijke Autenrieth	generic (EDICO SK)	Geomagic Studio 10	0,2	2,6	0,3	39562919	750000

Surface reconstruction was done twice by different users via isosurface rendering. JMF extracted one 3D surface of each the anterior and posterior half of the cranium after registration but before transformation of the image stacks using Amira 5.0 (thresholds were 13,500 and 15,200, respectively). Both anterior and posterior surfaces were cleaned of internal surfaces that are naturally generated by threshold-based surface extraction from CT data, and merged into a single 3D surface in GOM Inspect V7.5 software (http://www.gom.com/de/3d-software/gom-inspect.html). MA extracted one complete 3D surface from the transformed image stacks in ZIB-Amira 2015.24 (developed by the Zuse Institute Berlin; threshold was 15,177.2) and used Geomagic Studio 10 software for post-processing. During post-processing, internal surfaces were removed by cutting the model in half, clearing out the interior, and stitching the model back together. Finally, in order to ensure comparability, polygon counts of both resulting 3D surface models were reduced to 750,000 in Geomagic Studio, and meshes were saved as .ply file format.

Photogrammetry

Photogrammetry is a method that uses photos of an object to calculate a 3D model, originally employed in mapping and architecture, and successively adapted for other fields of science. Camera setup and photo alignment used to be rather complicated procedures, relying on the principle of triangulation (e.g., Wiedemann et al., 1999), but with steady progresses in computer technology, photogrammetry has become a simple, quick and inexpensive method for 3D reconstruction. For a review of the method see Falkingham (2012).

Photogrammetry is now widely used in paleontology, and reviews addressing its application in paleontological contexts conclude that overlap and consistent lighting and focus are the most crucial points for taking suitable photos (Fahlke et al., 2013; Fahlke, 2014; Mallison and Wings, 2014).

For this study, overlapping high-resolution photos of the dorsal and ventral sides of the cranium were taken with a hand-held Canon EOS 650D digital SLR camera (5184 x 3456 pixels). Photos were taken while walking around the specimen, and no turntable was used. In order to distinguish this method from automated photography, we are referring to it here as "manual photogrammetry".

Three sets of photos were taken by different people but processed by the same user. The set taken by MA comprised of 484 photos (198 from dorsal perspectives, 286 from ventral perspectives) of which 378 were used in alignment, with white balance (WB) set to tungsten light, using a 50 mm fixed object lens and an external RF550 Macro LED ring flash. The set taken by Heinrich Mallison (HM, Museum für Naturkunde Berlin) comprised 150 photos (46 from dorsal perspectives, 104 from ventral perspectives), using an object lens with 18-135 mm focal length, automatic WB, and the built-in flash. For this set, the camera was held upside-down to light the naturally shaded areas and thus to avoid hard shadow. The set taken by JMF comprised 83 photos (41 from dorsal perspectives, 42 from ventral perspectives), with WB set to fluorescent light, using a fixed 50 mm lens and no flash light. Sensitivity (ISO) was constant at 200 and depth of field was automatic in all three sets.

Individual 3D surface models were generated from all sets of photos by MA in Agisoft PhotoScan Professional 1.2.0, using high accuracy. Models were also scaled in PhotoScan based on a scale placed next to the cranium and included in the photos. Scaling was subsequently verified by measuring the condylo-basal length of the model in MeshLab v1.3.1 (http://meshlab.sourceforge.net/) and comparing it to the known condylo-basal length of the original cranium. Post-processing was done in Geomagic Studio for all models. During post-processing, holes were fixed, and redundant polygons were removed. In a last step, polygon counts were reduced to 750,000, and meshes were saved in .ply file format.

For automated photogrammetry we used the MDS Witikon technology provided by EDICO SK, Bratislava, Slovakia, that is usually used to create so-called object panoramas. Witikon is a system that makes use of four suspended high-resolution cameras that are automatically positioned and calibrated. For the particular photos of our specimen, four PHASE ONE IQ1 40 megapixel cameras with PHASE ONE AF Macro 120mm/4 lenses were used, and light provided by four external stationary FOMEI DIGITAL PRO 1200X flashes. The cranium was placed on a turntable which was rotated in six-degree increments so that 288 photographs were taken from each the dorsal and ventral side. Color calibration, alignment of the photographs and scaling were performed by EDICO staff using their generic company software. The reconstructed surface that was then provided for download consisted of 39.6

Table 2 - Surface models used in comparisons, and motivation for comparisons.

Comparison	Reference surface	Registered surface	Aspect addressed by comparison	Note	Shown in
1	P_MA	CT_MA	differences between methods	different methods, same user	Figure 2
2	CT_MA	CT_JMF	inter-user differences	same method, same dataset, different users	Figure 3
3	P_MA	P_HM	differences between data collectors	same method, different data sets, same user	Figure 4
4	P_MA	P_JMF	differences between data collectors	same method, different data sets, same user	Figure 5
5	P_MA	WITI	differences between methods	manual vs. automated photogrammetry	Figure 6

million polygons and was reduced by MA to 750,000 polygons using Geomagic Software.

The object panorama of MB.Ma. 51832 created and hosted by EDICO SK can be accessed at http://short.edico.sk/short/bothriodon/58386f (last accessed October 20, 2015).

Comparison

We conducted five surface comparisons using CloudCompare v.2.6.1 and v.2.6.2 beta (http://www.danielgm.net/cc/; software downloaded July 27, 2015). These comparisons are listed in Table 2. CloudCompare was chosen for all comparisons because it provides excellent registration and visualization features, as well as simple statistical tools for evaluation. Furthermore, researchers can address their questions directly to the developer, Daniel Girardeau-Montaut (Grenoble, France), at http://www.danielgm.net/cc/forum/ (last acces-sed October 28, 2015).

In CloudCompare, two point clouds or 3D surfaces are aligned, one representing the reference, and the other one being registered to it. The distance of these two point clouds or surfaces is measured at an arbitrary number of points (the size of the cells in which the nearest point is determined is usually pre-set by CloudCompare but can be changed by the user by manipulating the so-called octree level). For all comparisons we used 20 iterations with a random sampling limit of 50,000, with rotation and translation but no re-scaling allowed during alignment, and recommended octree level 8.

The five comparisons address various aspects in regard to the methods used: In order to test the feasibility and accuracy of Micro-CT scanning as opposed to manual photogrammetry, two surfaces generated from respective data sets produced by the same person (MA) were compared. Reproducibility (inter-user error) was tested using surfaces generated from the same micro-CT dataset by different users (MA and JMF), each choosing surface extraction settings intuitively. Furthermore, reproducibility from datasets that were created by different people (MA, HM, JMF) using individual settings of the same method (manual photogrammetry), and processed by the same user (MA), was addressed. Last, a surface generated with manual photogrammetry was compared with one generated using an automated setup (Table 2). Results of all surface comparisons are listed in Table 3 and shown in Figures 2-6.

Table 3 - Comparison results: mean, standard deviation, and largest distances between surfaces.

Comparison	Reference surface	Registered surface	Mean distance (mm)	Standard deviation σ (mm)	Mean - 2σ (mm)	Mean + 2σ (mm)	Largest negative distance (mm)	Largest positive distance (mm)
1	P_MA	CT_MA	-0,3148	1,1577	-2,6302	2,0006	-11,4815	6,6776
2	CT_MA	CT_JMF	-0,3346	1,6357	-3,6060	2,9368	-14,3785	11,7787
3	P_MA	P_HM	-0,1926	0,6613	-1,5152	1,1300	-9,8166	5,5856
4	P_MA	P_JMF	-0,3077	0,9823	-2,2723	1,6569	-11,3428	7,4464
5	P_MA	WITI	-0,1318	0,7123	-1,5564	1,2928	-11,3444	4,0871

RESULTS

In order to compare the efficiency of the different methods, durations of data collection, surface generation, and post-processing as well as polygon counts of the output surfaces were documented and are listed in Table 1. Quantitative and visual comparisons were conducted between two surfaces at a time. Below, distances of the respective registered surface from the reference surface are shown and discussed. Positive distances mean that points of the registered surface lie above, i.e., outside of the reference surface, whereas negative distances refer to points below, i.e., inside of the reference surface. In the illustrations (Figures 2-6), positive deviations are shown in yellow to red colors, negative deviations are shown in blue to purple colors, and areas with virtually complete consistency of the two surfaces are shown in green. The same color scale applies for all comparisons.

In the comparison of surfaces generated with different methods, namely micro-CT scanning and manual photogrammetry (Figure 2), CT_MA deviated from P_MA by -0.31 mm on average, with 95% of the distance measurements falling between -2.63 and 2.00 mm. Largest deviations were recorded at -11.48 and 6.68 mm (Table 3, Figure 2C). Largest negative distances occurred on the medial surface of the squamosals and

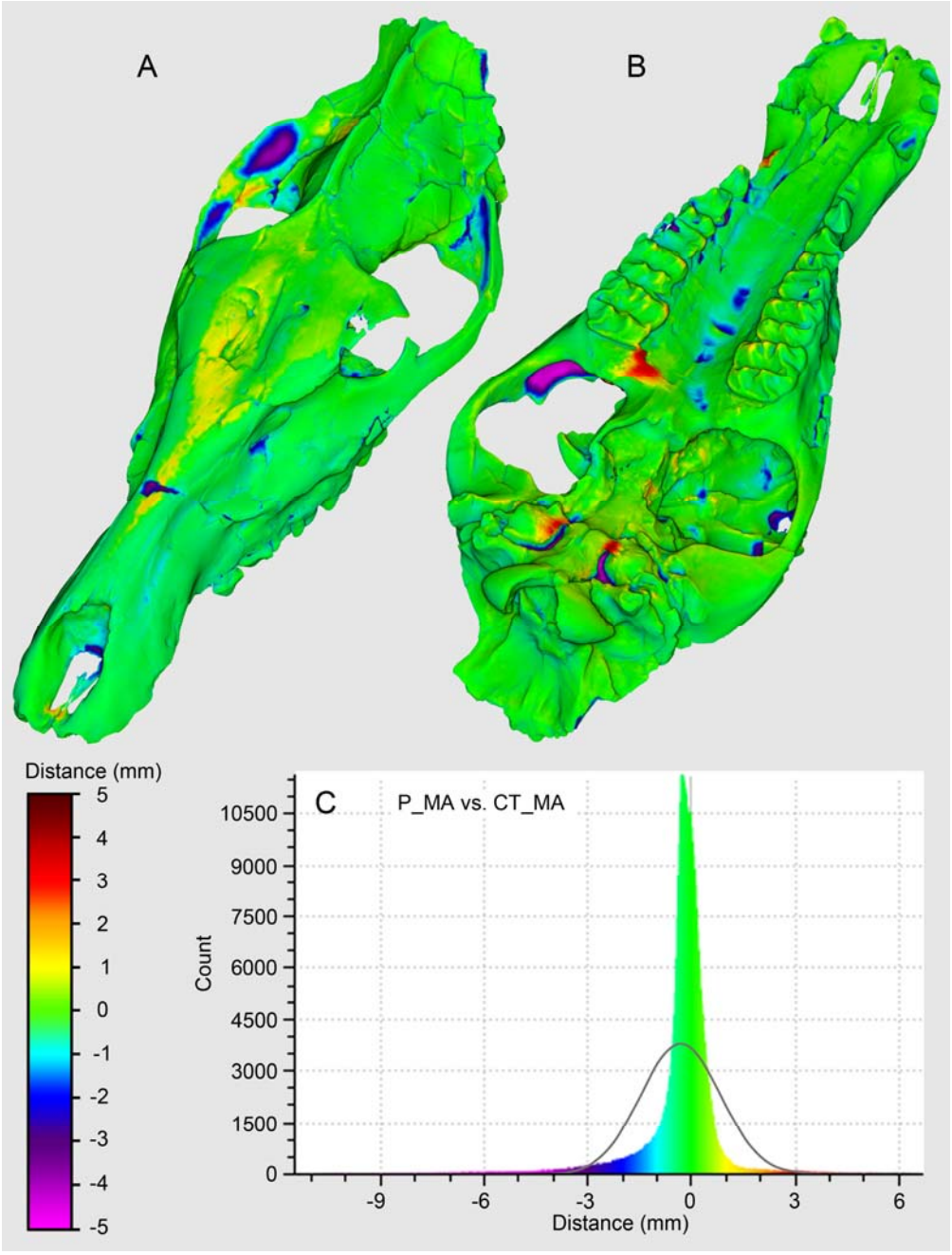

Figure 2 - Comparison of the surfaces P_MA generated by means of manual photogrammetry and CT_MA generated from micro-CT scans. A) Anterodorsal view. B) Posteroventral view. C) Distribution of distances between surfaces based on 612 classes. Gauss curve superimposed on histogram.

inside a crack across the nasals, as well as on the medial side of both zygomatic bones, in some depressions along the ventral midline suture of the maxillae, and in the jugular notch posteromedial to the tympanic bulla. Largest positive deviations were seen on the dorsal side of the frontal and nasal bones, on the zygomatic processes of the squamosals, and on what appears to be artificial bridges between the tympanic bullae and the basioccipital, and between the right maxillary and the palatine (Figure 2A,B). Parts of the nuchal crest and the supraorbital process of the frontal were missing in this comparison.

Comparing the results of surface extraction from the same CT dataset by different users (Figure 3), mean distance and largest distances between CT_MA and CT_JMF, as well as the standard deviation, were the largest recorded in all comparisons. Average deviation of CT_JMF from CT_MA was -0.33 mm. 95% of the distance measurements fell between -3.60 and 2.94 mm, with the largest distances at -14.38 and 11.78 mm, respectively (Table 3, Figure 3C). These extreme values are surprising in the light of the almost all-green comparison indicating a high degree of similarity of both surfaces (Figure 3A,B), a matter that will be

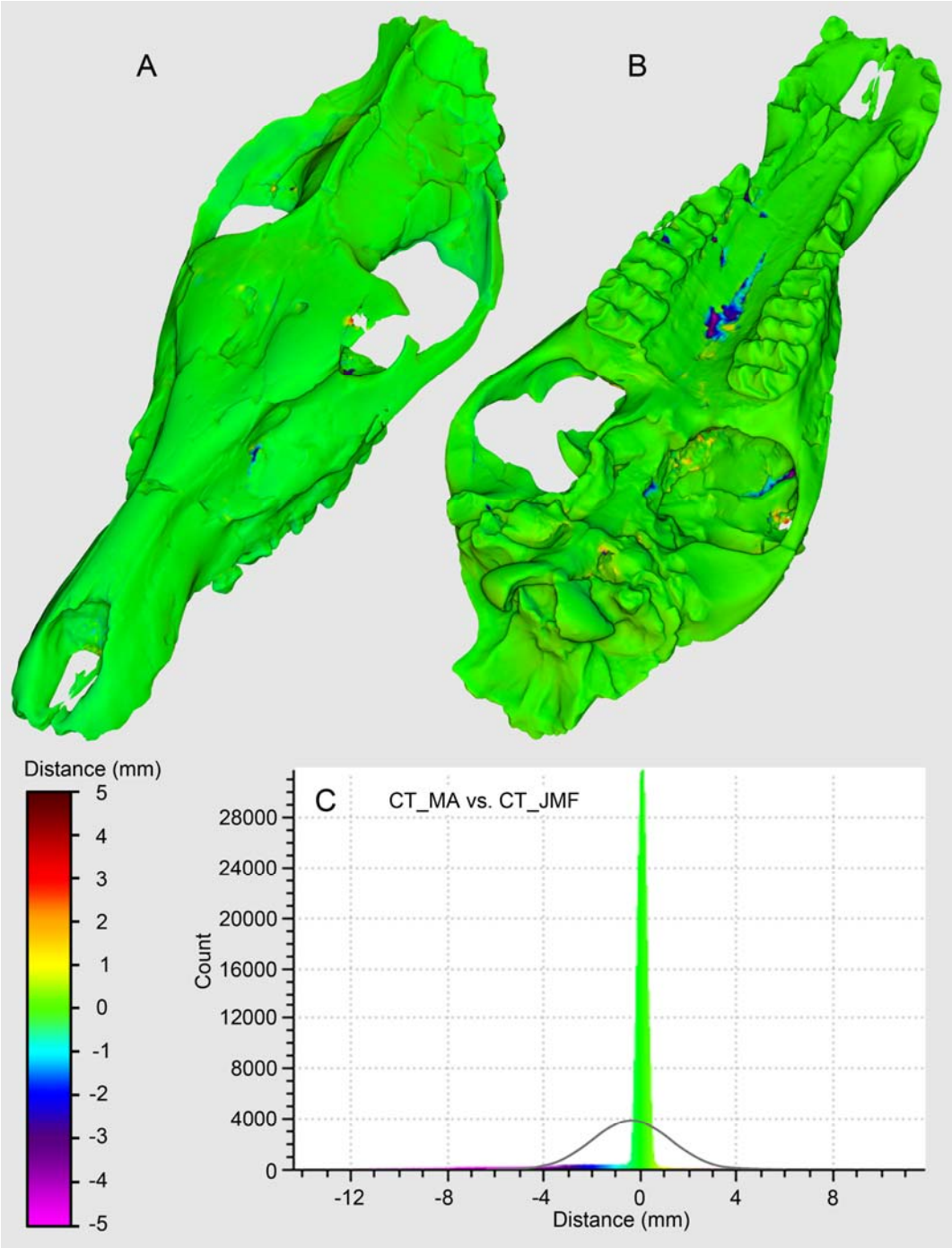

Figure 3 - Comparison of the surfaces CT_MA and CT_JMF generated from micro-CT scans. A) Anterodorsal view. B) Posteroventral view. C) Distribution of distances between surfaces based on 612 classes. Gauss curve superimposed on histogram.

further elaborated on in the Discussion. Greatest negative distances on the surface occurred on the ventral side of the maxillae and in crevasses on the ventral side of the supraorbital process of the left frontal, whereas the largest positive distances could be found in small, possibly artificial mounds emerging from the surfaces of the pterygoid and sphenoid bones. The artificial bridges between the tympanic bullae and the basioccipital, and between the maxillary and the palatine seen in the previous comparison were present in this comparison as well, however, they were mostly green here, indicating no differences between the two surfaces. Again, parts of the nuchal crest and the supraorbital process of the frontal were missing in this comparison.

In both comparisons of surfaces generated from different sets of photographs, the surface based on the largest set of photographs (P_MA) served as a reference surface to which the surfaces derived from an intermediate number of photos (P_HM) and from a small number of photos (P_JMF) were compared.

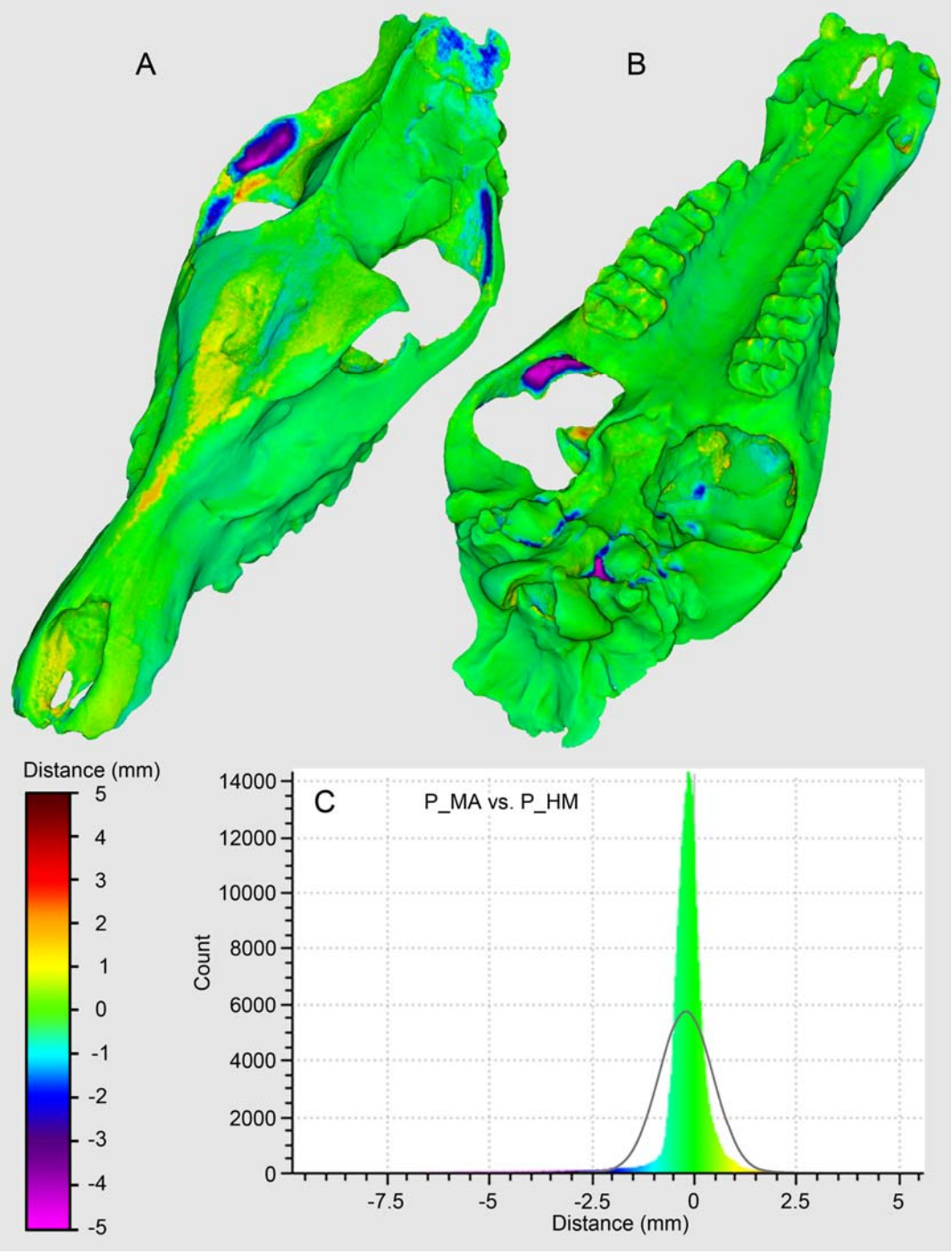

Figure 4 - Comparison of the surfaces P_MA and P_HM generated by means of manual photogrammetry. A) Anterodorsal view. B) Posteroventral view. C) Distribution of distances between surfaces based on 612 classes. Gauss curve superimposed on histogram.

In the first of these comparisons (Figure 4), P_HM deviated from P_MA by -0.19 mm on average. 95% of the distance measurements lay between -1.51 and 1.13 mm, reflecting the smallest standard deviation of all comparisons. The greatest distances between these surfaces, -9.82 and 5.59 mm, were also the smallest recorded throughout the analysis (Table 3, Figure 4C). Largest negative deviations of P-HM from P_MA could be found on medial surface of the squamosals and of the zygomatic bones, and in the jugular notch, and largest positive deviation appeared in the dorsal region of the frontal and nasal bones and on the zygomatic processes of the squamosals, resembling the comparison between P_MA and CT_MA. Additional large negative distances occurred dorsally towards the nuchal crest, and large positive distances on the tips of some teeth, on the ventral side of the right supraorbital process, and on the lateral surfaces of the sphenoid and frontal bones (Figure 4 A,B). Note that the nuchal crest, the nasal and the supraorbital processes were as complete as in the original cranium (Figure 1), and there were no depressions on the ventral side of the maxillae and no bridges connecting the petrosal and the basioccipital, and the maxillary and the palatine in this comparison.

In the second manual photogrammetry comparison (Figure 5), P_JMF deviated from P_MA

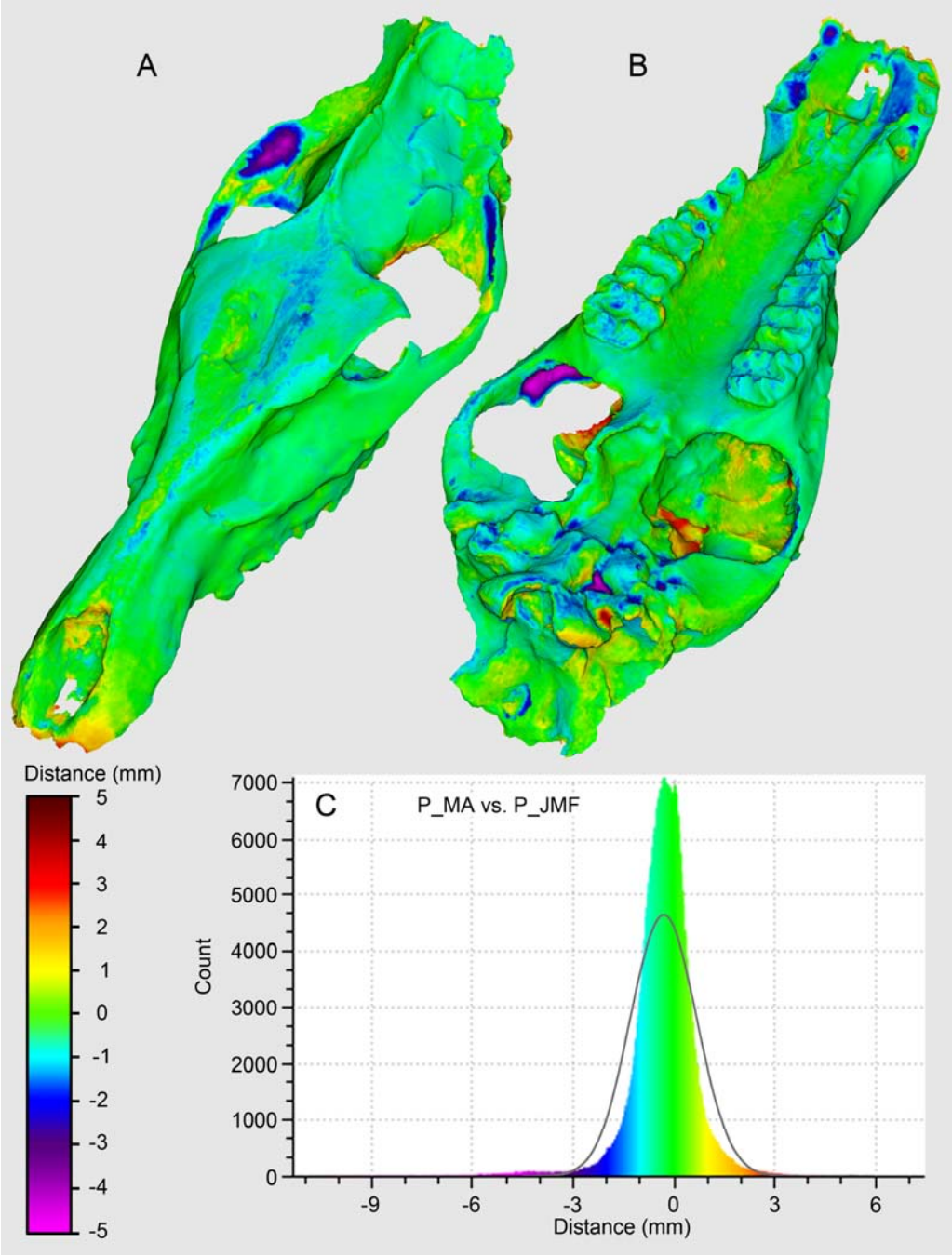

Figure 5 - Comparison of the surfaces P_MA and P_JMF generated by means of manual photogrammetry. A) Anterodorsal view. B) Posteroventral view. C) Distribution of distances between surfaces based on 612 classes. Gauss curve superimposed on histogram.

by -0.31 mm on average. Medium standard deviation yielded 95% of the distance measurements between -2.27 and 1.66 mm, with largest distances at -11.34 and 7.45 mm, respectively (Table 3, Figure 5C). Visually, this comparison revealed strong positive and negative deviations close to one another (Figure 5 A,B). As in the other comparisons involving P_MA as the reference surface, largest negative deviations of were recorded on medial side of the squamosal and of the zygomatic bone, and in the jugular notch adjacent to the tympanic bulla. Additional notable negative deviations of P_JMF from P_MA were on the dorsal side of the frontal and nasal bones, in several places across the basicranium, on the tooth cusps of the cheek teeth, on the ventral side of the left premaxilla, in the alveoli of the right incisors and canine, and on the labial side of the only present incisor in the right premaxilla. Largest positive distances could be found on the anterodorsal portion of the rostrum, particularly on the anterior rim of the premaxillae, on the squamosals, on the occipital, especially on the posterior surface of the occipital condyles, and on the ventral (orbital) side of the frontals. Again, the cranium was complete in this comparison, lacking artificial grooves or bridges.

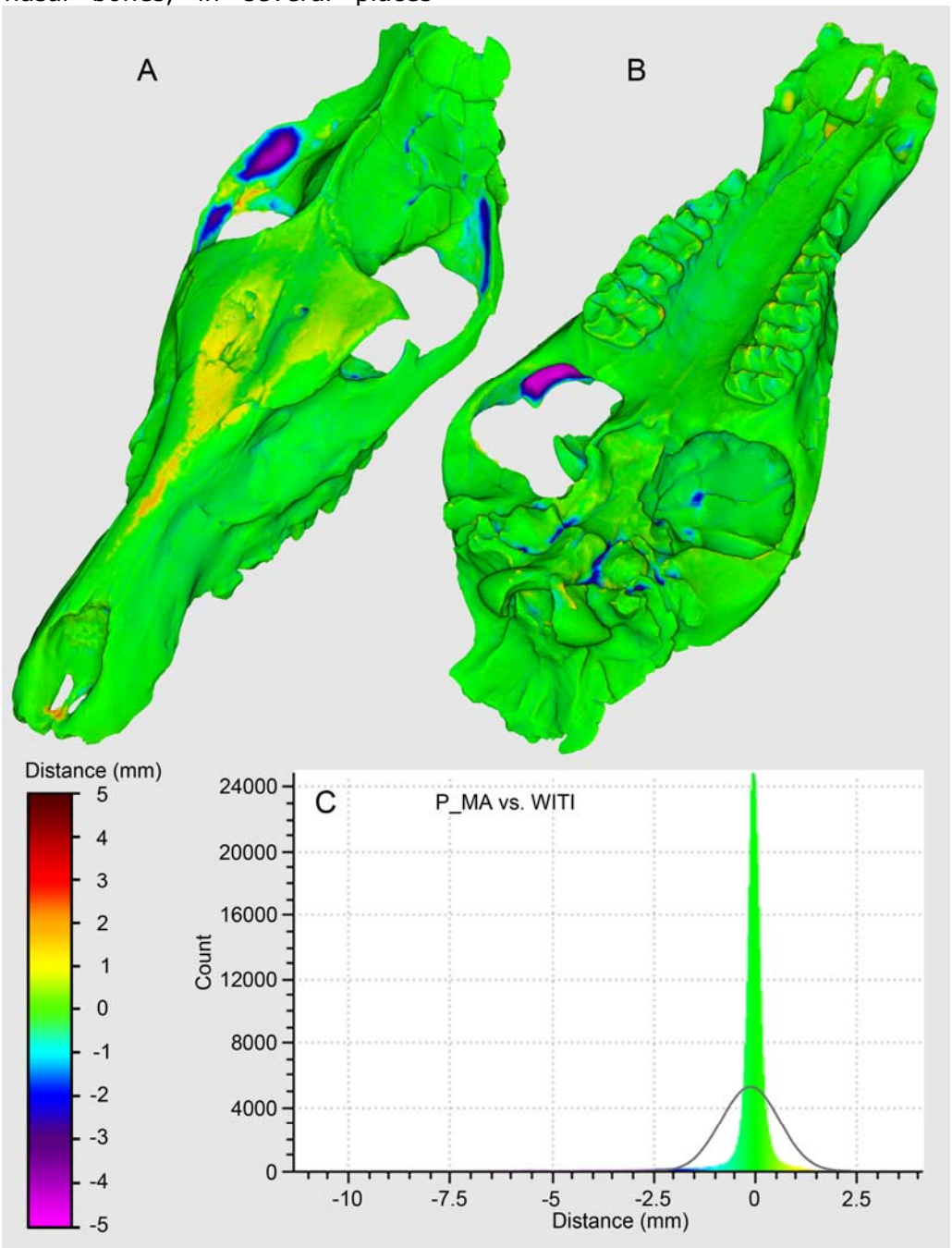

Figure 6 - Comparison of the surfaces P_MA generated by means of manual photogrammetry and WITI generated using automated photogrammetry. A) Anterodorsal view. B) Posteroventral view. C) Distribution of distances between surfaces based on 612 classes. Gauss curve superimposed on histogram.

Quality differences of manual and automated photogrammetry were analyzed comparing P_MA and WITI (Figure 6). Mean distance of WITI from P_MA was -0.13 mm, the smallest mean distance of the entire analysis. 95% of all distance measurements fell between -1.56 and 1.29 mm, and the largest distances between the two surfaces were recorded at -11.34 and 4.09 mm (Table 3, Figure 6C). Again, the largest negative distances were on the medial surfaces of the squamosals and zygomatics, and in the jugular notch, while the largest positive distances occurred on the dorsal surfaces of the frontals and nasals, and on the zygomatic processes of the squamosals. Further positive deviations of WITI from P_MA were seen on some tooth cusps, near the medial suture and inside a crack on the ventral side of the premaxillae, in the alveolus of the right canine, and, notably, on some crest-like elevations on the ventral side of the occipital condyles (Figure 6A,B). Besides these elevations, no artificial surface structures were noticed on the complete cranium in this comparison.

DISCUSSION

Here, we will discuss accuracy, efficiency and reproducibility of the methods used in this study. Strengths and weaknesses of the individual methods with regard to their application in 3D surface generation are summed up in Table 4.

Table 4 - Strengths and weaknesses of the tested methods with regard to 3D surface generation only.

Method	Original use	Strenghts in 3D surface generation	Weaknesses in 3D surface generation
Micro CT	Visualization of internal structures, medical applications	High detail resolution (sharp edges, etc.) Automated scaling Not much learning required for surface extraction	Much more data produced than needed remainders of internal structures artificially increase surface size Potentially high inter-user error due to internal structures Deletion of less dense portions due to threshold separation No surface color Long scanning time Long surface generation time Long post-processing time Expensive
Manual photogram-metry	Measurements using triangulation, surface reconstruction	Sufficient detail even with few photos Surface color Fast data acquisition Relatively short post-processing time Very versatile Cheap High reproducibility	Manual scaling Potentially long surface generation time in case of many photos (time consuming calculations) Time-consuming learning and practice required
MDS Witikon (automated photogram-metry)	Online object panoramas	high-quality calibrated surface color Very short data acquisition time Short surface generation time (easier calculations than with manual photogrammetry due to fixed camera positions) Very short post-processing time External data collection and processing: time-efficient for user External data collection and processing: no learning or practice required	Manual scaling Extremely large surfaces files External data collection and processing: no control over settings Expensive

Accuracy

Accuracy of a 3D surface basically refers to the highest possible degree of similarity between the 3D surface model and the original specimen. One aspect in terms of accuracy is certainly the maximum possible resolution. "Resolution" should not be used synonymously with "polygon count", because there may be redundant polygons in a mesh. However, if we are looking at cleaned meshes, minute anatomical features are usually resolved more accurately the higher the polygon count in the respective area of the surface. So, overall polygon count potentially influences resolution. Since computing technology is constantly improving, it is certainly advisable to collect data at the highest possible quality, e.g., use the best available camera resolution, and to store the original large files, such as surfaces with high polygon counts, for later use. However, for transport (email, upload) and manipulation with morphometric or modeling software, usually decimated meshes with smaller polygon counts are used.

Maximum polygon count of the generated surface prior to decimation (Table 1) was highest in automated photogrammetry where the cleaned surface provided for download was 39.6 million polygons. Witikon initially produced a model with an even higher count at 185 million polygons which we did not use in this study due to the very large file size of 3.72 GB. Using regular office computers (4 GB and 16 GB RAM, 3.3 GHz and 3.1 GHz processor, respectively) and common post-processing software (MeshLab and GOM Inspect), it was hardly possible to open this file and impossible to manipulate it. And not every researcher or working group is equipped with computers with suitable processors and memory for dealing with files this size. So while high polygon counts might impact resolution, and high resolution is definitely wanted in a 3D model that is supposed to be used for morphological analyses, file size and computing capacity are limiting factors. Additionally, when using any kind of photogrammetry, it does not make sense to produce and use 3D surfaces that have a higher polygon density than the pixel density of the photographs used for model generation. This kind of artificially high resolution would be misleading to the user and would not add to the true quality of the surface in question.

In our experience, 3D surfaces out of PhotoScan based on manual photogrammetry, provide by far enough detail for subsequent morphological analysis, regardless of whether the output is the maximum polygon count (P_HM, 3.2 million polygons) or limited to 1 million (P_MA, P_JMF). Even in the surfaces downsized to 750,000 polygons, morphological details are clear and crisp, and file size is very handy at approximately 14 MB. Of course, the desired accuracy of morphological detail depends on the purpose of the 3D surface. If small features need to be resolved in great detail, image resolution should be high to begin with, and additional close-up photos of the area in question will be more useful than a high overall polygon count. One should also keep in mind that resolution is determined by number of polygons (or vertices) per surface unit, which means that object size should be considered when choosing the desired total number of polygons in its 3D surface.

Scaling is another factor that influences the similarity of a 3D surface and the original object. False scaling can lead to invalid measurements, and thus, depending on the kind of study, flawed morphometric statistics or even wrong species assignment. The only method in our study that provided automatic scaling was micro-CT scanning. Varying between common file formats usually provided by scanning facilities, voxel size is usually either included in the file information or automatically recorded so that it can be entered manually when opening the data. Thus, exact scaling of the resulting surface model is ensured. In manual as well as automated photogrammetry, usually a physical scale is included in the photographs. For scaling, two points on this scale are picked manually in several photographs (the more the higher the accuracy of the scale), and the known distance between these points is typed in. Since it is not simple to mark the exact same points every time, if, e.g., the area is blurred in one photograph and cast in shadow in another, this procedure bears quite some potential for errors (in addition to potential mistakes typing in the distance) that may lead to imprecise or incorrect scaling of the surface model.

In search of differences between the digital surfaces and the original cranium, and between individual digital surfaces, some artificial features were readily identifiable in our study. These include the occurrence of bridges between the tympanic bullae and the basioccipital, and between the right maxillary and the palatine in both CT-generated surface models (CT_MA and CT_JMF; Figures 2 and 3). These features were not visible in any other surface model, and they are not part of the original cranium (cf. Figure 1B). We interpret them to be the results of scanning artefacts:

there appear to be extremely densely mineralized areas in these regions of the tympanic bullae, appearing very bright in the images of the image stack provided by the scanning facility. There are notable halos around these bright spots, extending toward the basioccipital.

In both CT-MA and CT_JMF, small parts of the cranium are missing, including parts of the nuchal crest and the supraorbital process of the frontal, as well as the filling of a crack across the nasals. These parts were lost during threshold-based surface generation in Amira. Apparently, these areas had been repaired during fossil preparation using adhesives and fillings with a lower density than the fossil bone. This low-density material appears darker in the CT scan and is deleted when the threshold for the gray value of the fossil bone is applied. If a bone fragment is glued back in place and is surrounded by lower-density material, it will be disconnected from the cranium in the surface reconstruction and accidentally be deleted during post-processing, which is what happened at the nuchal crest of our specimen.

Further artificial structures that are not part of the original cranium are ridges on the ventral side of the occipital condyles in the 3D model generated by automated photogrammetry (WITI) and stand out in its comparison with P_MA (Figure 6B). These ridges mark the places in which the cranium was touching the turntable when the photos of the dorsal side were taken. In photogrammetry, these contact points between an object and the surface underneath (that is usually deleted from the point cloud or model), are sometimes reconstructed as transitions. The results of this kind of reconstruction error are bumps and ridges on the 3D surface parallel to the area of contact. Correct reconstruction of these contacts is especially difficult, if they lie in the shade in the photographs, or if the object and the supporting surface have similar colors. Possibly, the latter was the case when automated photogrammetry was applied to MB.Ma. 51832, as the bright beige color of the fossil bone (Figure 1) was not a strong contrast to the white of the turntable that was used to rotate the specimen.

Reproducibility and efficiency

By reproducibility we are referring to the ability to produce consistent 3D surfaces, either by using different methods or by different people applying the same method in different ways. Reproducibility was generally very good: mean distance between two surfaces was 0.33 mm or less in all comparisons, which is less than 1‰ of the length of the cranium (37.5 cm). Furthermore, in all comparisons, 95% of all distance measurements were within 1% of the cranium length (Table 3).

As discussed above, parts of the surface of the original cranium that were made of less dense material (glue, plaster filling) were not reconstructed in the 3D surfaces based on micro-CT scanning. Therefore, although mean distance and standard deviation were comparable, reproducibility between Micro-CT scanning and manual photogrammetry could be regarded as lower than reproducibility between manual and automated photogrammetry, or between various data sets when manual photogrammetry was applied. Reproducibility within methods (i.e., inter-user differences or differences based on the settings used in data collection) is addressed in the discussion of the individual methods below.

Efficiency is defined here as the balance between the time and money invested in surface generation and the amount of usable data produced when using a certain method.

One general aspect in terms of efficiency of a method is the time required for learning and practice before a method can be applied by the researcher at all. Part of the purpose of this study was the evaluation of this learning process. Therefore, one of the authors (MA), who had no previous experience with 3D surface generation, documented the time and effort needed. Training and practice are not an issue when using the Witikon automated photogrammetry setup, because data generation and processing are completely outsourced to EDICO SK. However, training time plays a major part when it comes to making a decision on whether to use (micro-)CT scanning or manual photogrammetry for surface reconstruction.

While with CT scanning, the fundamental data are almost always produced by specialized staff at scanning facilities, researchers using photogrammetry mostly produce these data, i.e., the photographs, themselves. Therefore, photogrammetry requires more learning effort and practice for this very first step toward a reconstructed 3D surface. Overlap, lighting, and focus play a major role in basic photogrammetry (i.e. Fahlke et al., 2013; Fahlke, 2014; Mallison and Wings, 2014). Taking photos from the wrong angles with insufficient overlap or bad lighting (i.e. too bright, hard shadows, etc.) can lead to difficulties in the subsequent alignment process. Therefore, practice is

needed, and it takes longer to take a suitable set of photos for a beginner than it does for a professional. Going back and taking another set of photos because of failed alignment can lead to frustration and immensely increased data acquisition time, if it is possible at all. Data acquisition time for P_MA listed in Table 1 is actually the time needed for the fourth set only. Three previous sets led to failed alignment, so it would be adequate to estimate the learning and practicing time to be another three hours of attempted data collection, as well as approximately another 12 hours of attempted alignment before successful application of photogrammetry. This does not include the time needed to get acquainted with new camera equipment or settings, since MA, at that point, had already been using the camera for several weeks.

All programs used for data processing, photo alignment, surface generation, post-processing, and surface comparisons require thorough introduction. However, some are easier to use than others. While Amira (for surface extraction from CT data) and CloudCompare (for surface comparisons) were perceived as being complex and not particularly intuitive at first, they provide detailed tutorials or manuals, and/or online support, which actually made them reasonably easy to use after about a day of training. PhotoScan, the only photogrammetry software used in this study, proved to be quite easy to use, once the possible settings are understood. This program makes it possible for the beginner to find the best settings for their purpose via trial and error, but to save time, an introduction by someone who is experienced with this program is recommended. Among the programs used for post-processing, Geomagic Studio was perceived as the most intuitive. However, it was the only post-processing program in this study that is not free. So in case of a tight budget, researchers might want to resort to either MeshLab or GOM Inspect that might require a slightly longer training period but will serve the purpose as well.

Other aspects of efficiency such as processing times, costs, and usability of the data produced shall be discussed in the respective sections on the individual methods below.

Micro-CT scanning

In this study, micro-CT scanning yielded very detailed 3D surfaces, except for the deletion of less dense material described above. This deletion is certainly a disadvantage, if completeness is crucial for whatever analysis the researcher has planned. However, it could be viewed as an advantage, if one only wanted to reconstruct the original fossil surface without plaster fillings or glue.

While manual and automated photogrammetry produce 3D surfaces featuring the photo-realistic surface color of the original cranium, 3D surfaces derived from (micro-)CT scans are generally not colored. Again, it depends on the purpose of the study if one perceives missing surface color as a disadvantage. For mere morphometric measurements or landmark analyses, uncolored surfaces certainly suffice, but for taphonomic analyses or display purposes, surface color might be needed, which excludes CT scanning as a means for surface reconstruction.

In addition to the desired external surface, micro-CT scanning yielded a lot of surface data that may be unwanted in 3D surface reconstruction: the surfaces of internal bony structures of the cranium. These additional surfaces increase file size and are often connected to the external surface, resulting in holes and intersecting polygons that need to be fixed for further manipulation of the model, especially for purposes like 3D printing. Therefore these surfaces of internal structures should be removed, if the focus is on the reconstruction of the external surface. This removal, however, is extremely time-consuming, as connections within the outer shell need to be cropped manually so that partial surfaces can be deleted, resulting in long post-processing times of 6.3 and 17 hours, respectively (Table 1). The easiest and fastest way to remove the internal structures from both of our CT-generated 3D models (CT_MA and CT_JMF) was to clear out the interior of two halves of the surface and subsequently merge these halves to form a single surface. This approach was used right away with CT_JMF. With CT_MA, a hole was cut into the palate first to remove internal surfaces in the anterior part of the cranium before cutting the 3D model in half along a frontal plane, and clearing out the partial surfaces as described above. Surprisingly, the sutures connecting the previously disconnected anterior and posterior portions of the CT-based models can hardly be traced on the models themselves and show no deviations from other 3D surfaces in the comparisons (Figures 2 and 3). However, deviations seen in grooves on the palate in these comparisons are a result of the hole that was cut into CT-MA in this place and later filled using a generic filling function in Geomagic Studio.

Of course, small bits of internal surfaces of both models remained, because these tended to be folded and connected to the external surface in a way that made complete removal impossible without destroying the external surface. Furthermore, polygons of CT_MA and CT_JMF were not the same due to different thresholds used in surface extraction. Therefore, manual cutting and filling of the holes was not quite identical in both models. The difference of these internal remainders and filled holes caused the large standard deviation and greatest distances between these two models (i.e., lowered reproducibility between users; Table 3), whereas the visual comparison of both CT-based 3D surfaces indicates a high degree of similarity based on the green color of the external surface (Figure 3).

Costs for the micro-CT scan of our particular specimen were 714 Euros at the time (2012), including tax, but excluding travel costs to the scanning facility. This makes Micro-CT scanning the most expensive digitization method in our study.

Manual photogrammetry

Reproducibility from different sets of photographs using manual photogrammetry was very good. Particularly the two surfaces based on a higher number of photos (P_MA and P_HM with 378 and 150 photos, respectively) are very similar, having the smallest standard deviation and smallest extreme distances from one another of all comparisons (Table 3).

P_JMF was less similar to P_MA because of strong positive deviations in the front and back of the cranium and negative deviations on the dorsal and ventral sides (Figure 5), meaning that P_JMF was dorsoventrally flattened compared to P_MA (and, consequently, the other 3D surfaces). This might be a result of different photo alignment settings: while generic pair selection was selected in PhotoScan during alignment for P_MA and P_HM, pair selection was disabled for P_JMF, because photo alignment had failed when using the generic setting. One reason for alignment difficulties may be the lower number of images (83 photos) used for the generation of P_JMF, leading to less overlap. However, in the majority of these photos, the whole specimen, or at least a large portion of it was captured, so overlap should not be an issue. Another possible reason may be that the area of overlap of the photos from the ventral and dorsal perspectives was poorly lit, because it was in the shade either way, with the cranium dorsal side up and ventral side up, and no flash light was used while taking these photographs.

The importance of proper lighting, camera settings and overlap for 3D model generation becomes all the more obvious when details of the surface comparisons are evaluated. For example, all 3D surfaces that were compared to P_MA deviated to the negative in the same places on the squamosal bones (Figures 2, 4-6). We interpret this as P_MA lying above the other surfaces in these areas due to automatic hole filling in PhotoScan, and attribute this effect to the mode of lighting used during photography, and possibly problems with image overlap. The photographs used for the generation of P_MA were taken with a ring flash and WB set to tungsten light. Thus the specimen was evenly lit, and hard shadows were eliminated. Additionally the images were themselves were quite dark, eliminating highlights as well. Therefore, naturally shaded depressions may have not have been picked up as such. Furthermore, these areas on the cranium are only captured in a few photos, making it possible that not enough information for correct surface reconstruction was gathered due to insufficient overlap.

Taken together, our evaluations suggest that the light, settings and technique used by HM were most effective: the internal flash with the camera held upside down for better illumination of the areas where the photos from the dorsal and ventral perspectives overlap, and automatic WB.

Data collection and post-processing times were much shorter with manual photogrammetry than they were with micro-CT scanning, and slightly larger than when automated photogrammetry was applied. Duration of surface generation from photographs approximately equaled that of surface generation from micro-CT data (Table 1). While regular office computers were used for surface generation from CT scans and all post-processing, we used a more powerful server computer for surface generation from photos in PhotoScan. This computer provides partitioned RAM for several users at the same time, providing us with up to 40 GB of RAM at a time. While photogrammetric surface generation was tested and is well possible on computers with 4 GB RAM, surface generation time would of course be even longer. It needs to be kept in mind here though, that photogrammetric surface generation in Photoscan, once started, does not require interaction until it is finished, allowing the researcher to accomplish other tasks in the meantime, whereas the researcher

needs to be present and alert during the whole time of image stack registration and surface extraction from micro-CT scans, making manual photogrammetry the more efficient method in this regard. Data collection times and surface generation (calculation) times naturally increase the more photographs are taken per set (Table 1).

Another advantage of manual photogrammetry is its versatility: no specimen transport is needed, and photographs can usually be taken inside the collections that house the respective specimen(s), independent of the equipment and technology available on-site. For CT-scanning or automated photogrammetry, either the specimen or the setup (usually quite heavy equipment) need to be transported, increasing the risk of damage to the specimen.

The actual costs of manual photogrammetry can only be roughly estimated. In our specific case, the costs for the Canon EOS 650D camera including equipment such as a camera bag, an additional 50 mm lens and extra storage were 1006 Euros. Experience with photogrammetry at the Museum für Naturkunde has shown that it is possible to take well over 100,000 photos with this particular camera model without any signs of wear-out failure. This puts us roughly at 0.01 Euros per photograph, i.e. at 1.50 Euros for the set containing the intermediate number of photos (P_HM, 150 photographs), not including the electricity needed for charging the batteries, etc. So if the researcher's budget is an issue for data generation, as it is oftentimes the case, especially for student researchers, manual photogrammetry would be the means of choice.

Automated photogrammetry

The 3D surface resulting from automated photogrammetry (WITI) was very similar to those generated with manual photogrammetry. In order to have the same reference surface in most comparisons, WITI was compared with P_MA here, resulting in the smallest mean distance recorded in all comparisons (Figure 6, Table 3). Further comparisons (not shown here to avoid redundancy) revealed, however, that WITI was actually most similar to P_HM among all used 3D surfaces. This result suggests that manual and automated photogrammetry produce similarly accurate 3D surfaces.

Surface resolution is extremely high when using MDS Witikon for surface reconstruction (Table 1), which is a result of the high-resolution cameras used in the setup. On the one hand, this high resolution makes for stunningly detailed object panoramas, the original purpose of this method. On the other hand, as stated above, 3D surface files generated from these photos are much too large to be handled with regular office equipment, so that polygon count needs to be reduced anyway, making this method actually slightly less efficient for 3D surface generation than manual photogrammetry.

Data collection time is lowest in automated photogrammetry, because the automatic setup ideally does not require human interaction or correction during photography. Also, surface generation time is very low (Table 1), because computational requirements are greatly reduced when camera positions are fixed compared to a handheld camera that changes positions between photographs.

The regular minimum costs for the generation of one object panorama with the Witikon technology are 135 Euros. In case of a 3D model consisting of a dorsal and a ventral set of photos, costs would amount to 270 Euros, which is less than half the price of the micro-CT scan, but still almost two hundred times as much as what is needed for manual photogrammetry. One needs to bear in mind, however, that the costs for using MDS Witikon include complete data processing, saving the researcher valuable time, and thus making this the most convenient method for the researcher.

CONCLUSION

In our study we compared manual and automated photogrammetry and micro-CT scanning in terms of accuracy, reproducibility, and efficiency in 3D surface generation of a typical vertebrate fossil. The following summary presents our conclusions and recommendations that are in general accordance with the recommendations made by Mallison and Wings (2014) and Sutton et al. (2014).

3D surface comparisons and documentation of processing and training times revealed that manual photogrammetry has a high degree of reproducibility and is the most efficient and least costly method of those tested, given that appropriate lighting and camera settings are chosen in order to ensure accuracy. Manual photogrammetry is generally recommended if only the external surface of a specimen is of interest to the researcher, and especially in case of a small budget. However, one needs to account for training and practicing time prior to the application of this method.

Automated photogrammetry yielded results similar to manual photogrammetry but larger data volumes. If one is interested in an online object panorama (presentation and curation purposes) or in a 3D surface, but does not have the time for practicing or data processing, MDS Witikon offers a convenient digitization method ranging in costs between manual photogrammetry and micro-CT scanning.

Generally, when using photogrammetry, background color should contrast the color of the specimen, allowing for correct distinction between the two during surface generation.

CT scanning (including micro-CT) has its strength in the reconstruction of internal structures. While it is possible to extract external surfaces from CT scans, extremely long post-processing times, lack of photo-realistic surface colors, and high costs make this method less suitable for external 3D surface generation than the other methods tested. (Micro-)CT scanning should only be used for external surface generation if no other means is available. We would also recommend the additional use of manual photogrammetry, even if CT scans are available, if both internal and external surfaces are to be digitized.

ACKNOWLEDGMENTS

First, we thank Oliver Hampe and Thomas Schossleitner (Museum für Naturkunde Berlin) for access to the specimen, and valuable background information and discussion. We also thank Irina Ruf (Senckenberg Naturmuseum Frankfurt am Main, formerly Steinmann-Institut Bonn) and Georg Oleschinski (Steinmann-Institut Bonn) for micro-CT scanning, and Daniel Baum (Zuse Institute Berlin) for discussing surface registration techniques in ZIB-Amira. Heinrich Mallison (Museum für Naturkunde Berlin) is thanked for taking one set of photos used for photogrammetry and for helpful suggestions. We furthermore thank René Guráň, Róbert Sičak, Paul Safko and Mira Silanova (EDICO SK, Bratislava) for digitizing our specimen with MDS Witikon, and Daniel Girardeau-Montaut (Grenoble, France) for constructive comments regarding the use of CloudCompare. Funding was provided by the Deutsche Forschungsgemeinschaft (DFG FA 889/2-1) and the Alexander von Humboldt Foundation (Feodor Lynen Return Fellowship for JMF in 2012).
Publication costs were covered thanks to a grant from Transmitting Science to the Journal of Paleontological Techniques.

REFERENCES CITED

Clark, J., Beerbower, J. R. and Kietzke, K. K. 1967. Oligocene sedimentation, stratigraphy, paleoecology and paleoclimatology in the big Badlands of South Dakota. Fieldiana: Geology Memoirs 5:160.

Fahlke, J. M. 2014. Generation of three-dimensional (3D) surface models of baleen whale skulls (Cetacea: Mysticeti) for morphometric analyses: possibilities and limits of photogrammetry. 10th North American Paleontological Convention, Gainesville, FL, USA, February 15-18, 2014. NAPC Abstracts. Paleontological Society Special Publication 13:171.

Fahlke, J. M., Mallison, H., Wings, O. and Schwarz-Wings, D. 2013. One fits all: using photogrammetry to solve diverse problems with large-sized paleontological objects. 73rd Annual Meeting of the Society of Vertebrate Paleontology, Los Angeles, CA, USA, October 30-November 2, 2013. SVP 2013 Program and Abstract Book (Supplement to the online Journal of Vertebrate Paleontology, October 2013):124.

Falkingham, P. L. 2012. Acquisition of high resolution three-dimensional models using free, open-source, photogrammetric software. Palaeontologia Electronica 15 (1): 15.

Janis, C. M. 1995. Correlation between craniodental morphology and feeding behaviour in ungulates: reciprocal illumination between living and fossil taxa. In: Thomason, J. J. (ed.) Functional Morphology in Vertebrate Paleontology. Cambridge: Cambridge University Press, 67-98.

Kron, D. G. and Manning, E. 1998. Anthracotheriidae. In: Janis, C. M., Scott, K. M. and Jacobs, L. L. (eds.) Evolution of Tertiary Mammals of North America. Volume 1: Terrestrial Carnivores, Ungulates, and Ungulatelike Mammals. Cambridge: Cambridge University Press, 381-388.

Lihoreau, F. and Ducrocq, S. 2007. Family Antracotheriidae. In: Prothero, D. R. and Foss, S. E. (eds.) The Evolution of Artiodactyls. Baltimore: The Johns Hopkins University Press, 89-105.

Mallison, H. 2011. Digitizing methods for paleontology: applications, benefits and limitations. In: Elewa, A. M. T. (ed.) Computational Paleontology. Berlin Heidelberg: Springer-Verlag, 7-43.

Mallison, H. and Wings, O. 2014. Photogrammetry in paleontology – a practical guide. Journal of Paleontological Techniques, 12(1): 31.

Sutton, M. D., Rahman, I. A. and Garwood, R. J. 2014. Techniques for Virtual Palaeontology. Chichester: John Wiley & Sons, 208pp.

Wiedemann, A., Suthau, T. and Albertz, J. 1999. Photogrammetric survey of dinosaur skeletons. Mitteilungen des Museums für Naturkunde Berlin, Geowissenschaftliche Reihe 2:113-119.

Additional images and material can be downloaded at http://www.jpaleontologicaltechniques.org/